Available online at www.sciencedirect.com
ScienceDirect
Journal of Solid State Chemistry 179 (2006) 3919–3925
JOURNAL OF SOLID STATE CHEMISTRY
www.elsevier.com/locate/jssc

Crystal structures and photocatalysis of the triclinic polymorphs of $BiNbO_4$ and $BiTaO_4$

B. Muktha[a], J. Darriet[b], Giridhar Madras[c], T.N. Guru Row[a,*]

[a]*Solid State and Structural Chemistry Unit, Indian Institute of Science, Bangalore 560 012, India*
[b]*Institut de Chimie de la Matière Condensée de Bordeaux (ICMCB-C.N.R.S), Université de Bordeaux 1, 87, Avenue A. Schweitzer, 33608 Pessac Cedex, France*
[c]*Department of Chemical Engineering Indian Institute of Science, Bangalore 560012, India*

Received 9 June 2006; received in revised form 24 August 2006; accepted 27 August 2006
Available online 7 September 2006

Abstract

The high-temperature polymorphs of two photocatalytic materials, $BiNbO_4$ and $BiTaO_4$ were synthesized by the ceramic method. The crystal structures of these materials were determined by single-crystal X-ray diffraction. $BiNbO_4$ and $BiTaO_4$ crystallize into the triclinic system $P\bar{1}$ (No. 2), with $a = 5.5376(4)$ Å, $b = 7.6184(3)$ Å, $c = 7.9324(36)$ Å, $\alpha = 102.565(3)^\circ$, $\beta = 90.143(2)^\circ$, $\gamma = 92.788\ (4)^\circ$, $V = 326.21\ (5)$ Å^3, $Z = 4$ and $a = 5.931\ (1)$ Å, $b = 7.672\ (2)$ Å, $c = 7.786\ (2)$ Å, $\alpha = 102.94\ (3)^\circ$, $\beta = 90.04\ (3)^\circ$ $\gamma = 93.53\ (3)^\circ$, $V = 344.59\ (1)$ Å^3 and $Z = 4$, respectively. The structures along the *c*-axis, consist of layers of $[Bi_2O_2]$ units separated by puckered sheets of $(Nb/Ta)O_6$ octahedra. Photocatalytic studies on the degradation of dyes indicate selectivity of $BiNbO_4$ towards aromatics containing quinonic and azo functional groups.

Keywords: Single-crystal X-ray diffraction; Crystal structure; Bismuth niobate; Bismuth tantalate; Photocatalysis

1. Introduction

$BiNbO_4$ and $BiTaO_4$ belong to the family of the $A^{3+}B^{5+}O_4$ compounds. The triclinic forms of $BiNbO_4$ and the iso-structural $BiTaO_4$ were synthesized at 1149 °C [1]. Both $BiNbO_4$ and $BiTaO_4$ undergo an irreversible orthorhombic–triclinic transition. The low-temperature orthorhombic form synthesized at 900 °C transforms to the triclinic high-temperature form at 1020 °C for $BiNbO_4$ and at 1150 °C for $BiTaO_4$ [2,3]. Single crystals of the orthorhombic form of $BiNbO_4$ were grown from a flux containing BiOF below 900 °C [4].

The first attempt towards structure determination of the high temperature triclinic form of $BiNbO_4$, was made by Keve and Skapski who reported the single-crystal X-ray structure in the $P\bar{1}$ space group with $a = 7.61\ (1)$ Å, $b = 5.53\ (6)$ Å, $c = 7.91\ (9)$ Å, $\alpha = 89.88^\circ$, $\beta = 77.43^\circ$, $\gamma = 87.15^\circ$ and $Z = 4$ [5]. Since the data was collected on a twinned crystal, an absorption correction was not applied. This resulted in negative thermal parameters for Bi(1) ($B = -0.01\ (8)$ Å^2) and the oxygen atoms, O(1), O(2), O(4), O(6) and O(7) [5]. Subsequently, the crystal structure of the iso-structural $BiTaO_4$ was obtained by Rietveld refinement using the structural parameters of $BiNbO_4$ [5] in the space group $P1$ [6]. In another report of the Rietveld refinement of $BiTaO_4$, Lee et al. [7] used the space group $P\bar{1}$, but obtained high standard deviations for the positional parameters of oxygen atoms and unacceptable bond distances from powder X-ray data. Subsequently, photocatalytic activity of the solid solution of the type, $BiTa_{1-x}Nb_xO_4$ in the range ($0 \leqslant x \leqslant 1$) [8,9] was reported.

As explained above, the structural reports on the high temperature forms of both $BiNbO_4$ and $BiTaO_4$ are ambiguous. Since $BiNbO_4$ and $BiTaO_4$ are potential photo-catalytic materials, an accurate structure determination of these materials becomes extremely important in order to co-relate the structure property relationships. In

*Corresponding author. Fax: +91 80 23601310.
E-mail address: ssctng@sscu.iisc.ernet.in (T.N. Guru Row).

0022-4596/$ - see front matter © 2006 Elsevier Inc. All rights reserved.
doi:10.1016/j.jssc.2006.08.032

this context, our objective was to re-determine the crystal structures of $BiNbO_4$ and $BiTaO_4$ by single-crystal X-ray diffraction. Further, photocatalytic degradation of dyes like Orange G (OG), Methyl violet (MV) and Alizarin green (AG) were studied in the presence of $BiNbO_4$ and $BiTaO_4$.

2. Experimental

2.1. Materials

Bi_2O_3, Nb_2O_5 and Ta_2O_5 (all of them obtained from Fluka, 99.9%) were dried at 600 °C before use. Dyes, Methyl Violet MS, Orange G (all from S.D. fine-Chem Ltd., India) and Alizarin cyanine Green (Rolex, India) were used as such. Water was double distilled and filtered before use.

2.2. Synthesis and crystallization

Polycrystalline samples of $BiNbO_4$ and $BiTaO_4$ were synthesized by the ceramic route from Bi_2O_3, Nb_2O_5 and Ta_2O_5 in stoichiometric quantities. The reaction mixtures were ground well in an agate mortar and heated in a platinum crucible at 1100 and 1200 °C for 24 h for the preparation of $BiNbO_4$ and $BiTaO_4$, respectively. Preliminary X-ray powder patterns recorded on a Philips X'Pert diffractometer confirmed the formation of a single phase in each case. Single crystals of the compounds were grown by the melt cooling technique. Pale yellow powder samples of $BiNbO_4$ and $BiTaO_4$ were melted at 1200 and 1350 °C, respectively, and then cooled slowly at the rate of 1 °C/h down to 900 °C and then furnace cooled to room temperature to obtain transparent crystals in each case.

2.3. Single-crystal X-ray diffraction

X-ray powder patterns of crushed single crystals of both the compounds were recorded to establish phase purity in each case. Single crystals of $BiNbO_4$ and $BiTaO_4$ selected based on the quality of diffraction were mounted on Bruker Nonius Kappa CCD and Bruker AXS Smart CCD diffractometers respectively. Intensity measurements in both cases were performed using graphite-monochromated Mo$K\alpha$ radiation at 298 K. The structures were solved by direct methods using SHELXS97 [10] and were refined using JANA [11]. The heavy Bi and (Nb/Ta) atoms were obtained by direct methods. Subsequent difference Fourier synthesis revealed all the remaining oxygen atoms in both the cases. The crystallographic data and details of single-crystal data collection are listed in Table 1. The atomic coordinates of $BiNbO_4$ and $BiTaO_4$ are listed in Tables 2a and b. Further details of the crystal structure investigations on $BiNbO_4$ and $BiTaO_4$ can be obtained from the Fachinformationszentrum Karlsruhe (FIZ) on quoting the numbers CSD 415850 and 415849.

Table 1
Crystallographic data for $BiNbO_4$ and $BiTaO_4$

Crystal data		
Empirical formula	$BiNbO_4$	$BiTaO_4$
Crystal habit (color)	Cylindrical, colorless	Cylindrical, colorless
Crystal size (mm)	$0.086 \times 0.131 \times 0.248$	$0.084 \times 0.073 \times 0.062$
Cell system, space group	Triclinic, $P\bar{1}$	Triclinic, $P\bar{1}$
Cell dimensions (Å/°)		
a	5.5376(4)	5.931(1)
b	7.6184(3)	7.672(2)
c	7.9324(36)	7.786(2)
α	102.565 (3)	102.94(3)
β	90.143(2)	90.04(3)
γ	92.788(4)	93.53(3)
Volume (Å^3)	326.21 (5)	344.59 (1)
Formula weight	365.9	453.92
D_x (g/cm^3)	7.4473	9.002
Z	4	4
$F(000)$	624	752
Scan mode	ω scan + ϕ scan	ω scan
θ_{max} (°)	39.98	27.96
Recording reciprocal space	$-10 \leqslant h \leqslant 10$, $-13 \leqslant k \leqslant 13$, $-13 \leqslant l \leqslant 13$	$-7 \leqslant h \leqslant 7$, $-9 \leqslant k \leqslant 8$, $-10 \leqslant l \leqslant 10$
Number of measured reflections	17 058	2710
Number of independent reflections	3799 [R(int) = 0.0669]	1469 [R(int) = 0.0536]
Absorption correction	Gaussian	Numerical
μ (mm^{-1})	57.21	82.567
Refinement	F^2	F^2
No. of variables	110	110
$R(F)$, w$R(F^2)$	0.0348, 0.0868	0.0411, 0.0893
GoF	1.26	1.23
Max/min $\Delta\rho$ e/Å^3	4.48/−2.18	2.57/−2.87

2.4. Photocatalytic experiments

2.4.1. Photochemical reactor

The details of the photochemical reactor employed in this study have been reported elsewhere [12]. A high-pressure mercury vapor lamp (HPML) (125 W, Philips, India) that radiated predominantly at 365 nm corresponding to the energy of 3.4 eV was used for the degradation reactions.

2.4.2. Degradation

Powder samples of $BiNbO_4$ and $BiTaO_4$ were used for the degradation reactions. The degradation reactions were performed in a photochemical reactor with various initial concentrations with a constant catalyst concentration of 1.0 kg/m^3. Samples were collected at regular intervals for subsequent analysis. Control experiments conducted without the catalyst under UV radiation and with the catalyst without UV radiation did not show any appreciable degradation indicating that both the catalyst and UV radiation are required for the degradation reactions. There was only about 1% reduction in the concentration of all compounds of interest when a solution of 25 ppm was

Table 2
Final atomic coordinates and equivalent thermal parameters (U_{eq}) of (a) $BiNbO_4$ and (b) $BiTaO_4$

Atom	Wyckoff site	Occupancy	x	y	z	U_{eq} (Å)^2
(a) $BiNbO_4$						
Bi(1)	2*i*	1	0.28062 (4)	0.83463 (3)	0.62529 (3)	0.00878 (6)
Bi(2)	2*i*	1	0.23707 (4)	0.87647 (3)	0.12599 (3)	0.00953 (6)
Nb(1)	2*i*	1	0.22503 (9)	0.34402 (6)	0.17940 (6)	0.00566 (10)
Nb(2)	2*i*	1	0.24367 (9)	0.32513 (6)	0.67849 (6)	0.00585 (10)
O(1)	2*i*	1	0.0026 (8)	0.1027 (5)	0.1774 (6)	0.0105 (10)
O(2)	2*i*	1	0.4439 (8)	1.1055 (5)	0.6744 (5)	0.0098 (10)
O(3)	2*i*	1	0.1626 (8)	0.3185 (6)	0.9471 (5)	0.0102 (10)
O(4)	2*i*	1	0.0788 (8)	0.5518 (6)	0.7312 (5)	0.0116 (10)
O(5)	2*i*	1	0.2985 (9)	0.3286 (6)	0.4514 (5)	0.0121 (11)
O(6)	2*i*	1	0.4359 (8)	0.5466 (6)	0.2203 (5)	0.0114 (10)
O(7)	2*i*	1	0.4642 (8)	0.1549 (6)	0.1472 (5)	0.0084 (10)
O(8)	2*i*	1	0.0389 (8)	0.8329 (6)	0.3616 (5)	0.0111 (11)
(b) $BiTaO_4$						
Bi(1)	2*i*	1	0.2688 (3)	0.6201 (3)	0.3815 (3)	0.0315 (7)
Bi(2)	2*i*	1	0.2139 (3)	−0.3340 (3)	−0.1132 (3)	0.0311 (7)
Ta(1)	2*i*	1	0.2739 (3)	0.1574 (3)	0.3058 (3)	0.0267 (6)
Ta(2)	2*i*	1	0.2590 (3)	0.1747 (3)	−0.1929 (3)	0.0284 (7)
O(1)	2*i*	1	0.066 (7)	0.938 (6)	0.284 (7)	0.058 (18)
O(2)	2*i*	1	0.344 (5)	0.183 (3)	0.574 (10)	0.012 (4)
O(3)	2*i*	1	0.511 (7)	0.390 (5)	0.312 (5)	0.040 (12)
O(4)	2*i*	1	0.035 (5)	0.348 (3)	0.350 (4)	0.025 (9)
O(5)	2*i*	1	0.461 (5)	0.662 (2)	0.129 (4)	0.019 (9)
O(6)	2*i*	1	0.411 (8)	0.933 (7)	0.755 (5)	0.054 (16)
O(7)	2*i*	1	0.059 (4)	0.407 (5)	0.832 (5)	0.030 (11)
O(8)	2*i*	1	0.195 (8)	0.158 (6)	0.041 (6)	0.068 (18)

stirred with the catalysts (at a loading of 1 kg/m^3) for 12 h in dark. Therefore, the actual concentration of the solution was taken to be the initial concentration for kinetic analysis. The optimal catalyst loading was found to be 1 kg/m^3 with no significant increase in the degradation of organics for higher concentrations of the catalysts. Hence, this catalyst concentration was used for all the photocatalytic degradation experiments. The reactions were carried out at natural pH conditions with the initial concentrations of 25 ppm for OG and AG and 10 ppm for MV due to high molar absorptivity.

2.4.3. Sample analysis

The degraded samples were filtered through Millipore membrane filters and centrifuged to remove the catalyst particles prior to analysis. The samples were analyzed in cells of length 1 cm using a Lambda 32, Perkin Elmer UV–visible spectrophotometer. The calibration for AG, OG and MV was based on Beer Lambert's Law at their maximum absorption wavelengths λ_{max} of 626, 475 nm and 582 nm, respectively.

3. Results and discussion

3.1. Crystal structures

$BiNbO_4$ and $BiTaO_4$ crystallize in the triclinic system $P\bar{1}$ (No. 2) with $a = 5.5376$ (4) Å, $b = 7.6184$ (3) Å, $c = 7.9324$ (36) Å, $\alpha = 102.565$ (3)°, $\beta = 90.143$ (2)°, $\gamma = 92.788$ (4)°, $V = 326.21$ (5) Å^3, $Z = 4$ and $a = 5.931$ (1) Å, $b = 7.672$ (2) Å, $c = 7.786$ (2) Å, $\alpha = 102.94$ (3)°, $\beta = 90.04$ (3)°, $\gamma = 93.53$ (3)°, V = 344.59 (1) Å^3 and $Z = 4$, respectively. The crystal structure of $Bi(Nb/Ta)O_4$ along the *c*-axis is shown in Fig. 1a. It consists of pseudo layers of $[Bi_2O_2]$ units connected to each other and surrounded by sheets of puckered NbO_6 octahedra. When viewed along the *c*-axis, the $[Bi_2O_2]$ units appear to be tilted to each other instead of a linear arrangement (Fig. 1a). The crystal structures of triclinic $Bi(Nb/Ta)O_4$ can be compared with those of their orthorhombic polymorphs (Figs. 1a and b). The orthorhombic polymorph (Fig. 1b) can be described as typical layers of $[Bi_2O_2]$ units linked by layers of interconnected $(Nb/Ta)O_6$ octahedra. It is iso-structural to the low temperature form of $SnWO_4$ [13]. Fig. 2 shows the arrangement of the layers of Bi_2O_2 units along the *b*-axis in the triclinic forms of $Bi(Nb/Ta)O_4$. The co-ordination of NbO_6 octahedra, around the $[Bi_2O_2]$ unit is shown in Fig. 3a.

The bond distances of $BiNbO_4$ and $BiTaO_4$ are listed in Tables 3a and b, respectively. The Bi(1) atom in $BiNbO_4$ forms a distorted BiO_7 polyhedron with O(1) (2.192 (4) Å), O(2) (2.167 (4) Å), O(2′) (2.934 (4) Å), O(4) (2.675 (5) Å), O(5) (2.703 (5) Å), O(7) (2.274 (4) Å) and O(8) (2.477 (4) Å) (Table 3a). Bi(2) also forms irregular BiO_7 polyhedra. It has five relatively short bonds with O(1) (2.195 (4) Å) , O(2) (2.348 (4) Å), O(3) (2.596 (4) Å), O(7) (2.386 (4) Å) and

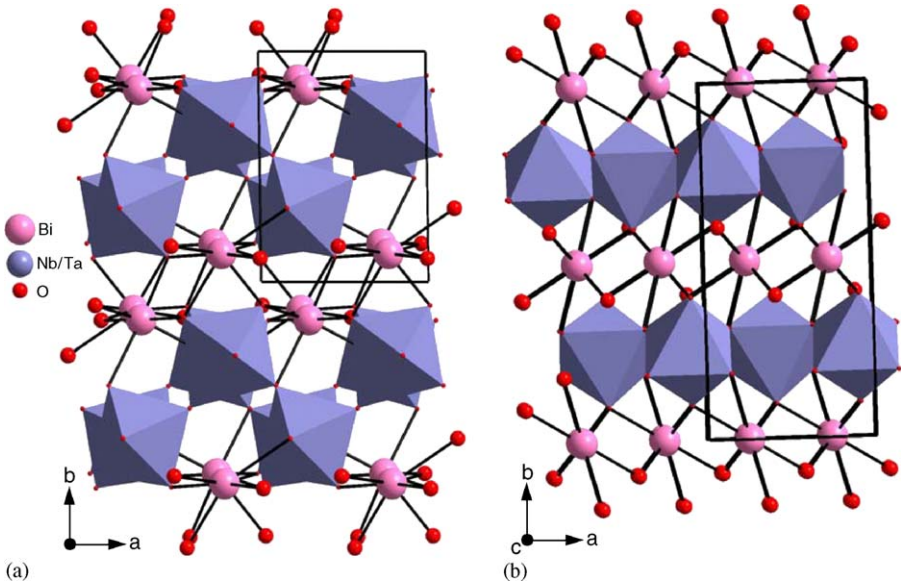

Fig. 1. Crystal structures of $Bi(Nb/Ta)O_4$ along *b*-axis: (a) triclinic form and (b) orthorhombic form.

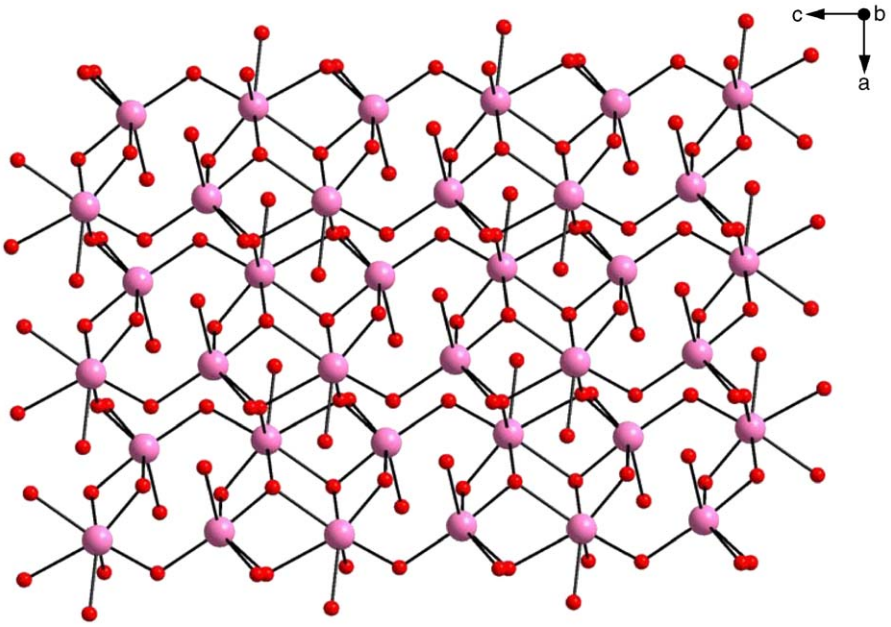

Fig. 2. The layers of Bi_2O_2 units in the triclinic form of $Bi(Nb/Ta)O_4$.

O(8) (2.248(5) Å) and two long bonds, O(1′) (2.770 (5) Å) and O(7′) (2.706 (4) Å). Each $[Bi_2O_2]$ unit in $BiNbO_4$ is surrounded by 10 NbO_6 octahedra of which five $Nb(1)O_6$ octahedra share edges and two $Nb(2)O_6$ octahedra share corners with the $[Bi_2O_2]$ unit. The Nb—O bond lengths are in the range (1.833–2.224 Å).

In $BiTaO_4$, both Bi(1) and Bi(2) form BiO_7 polyhedra. Bi(1) has four short bonds with O(3) (2.32 (4) Å), O(4) (2.40 (2) Å), O(5) (2.35 (3) Å), and O(7) (2.53 (3) Å) and three long bonds with O(2) (2.65 (3) Å), O(3′) (2.74 (4) Å) and O(4′) (2.74 (3) Å) (Table 3b). Bi(2) forms four short bonds with O(3) (2.24 (4) Å), O(4) (2.34 (3) Å), O(5) (2.40 (3) Å) and O(7) (2.09 (4) Å) and three long bonds O(6) (2.69 (5) Å), O(7′) (2.86 (4) Å) and O(8) (2.84 (5) Å). Each $[Bi_2O_2]$ unit is surrounded by eleven TaO_6 octahedra. Two $Ta(1)O_6$ octahedra and three $Ta(2)O_6$ octahedra share their edges with the $[Bi_2O_2]$ unit. The average Ta–O bond lengths are higher than the Nb–O bond lengths resulting in an increase in volume for $BiTaO_4$ (Table 1). The high esds observed in case of $BiTaO_4$ (Tables 2b and 3b) may be attributed to the poor crystal quality. Repeated attempts to grow better crystals of $BiTaO_4$ were unsuccessful.

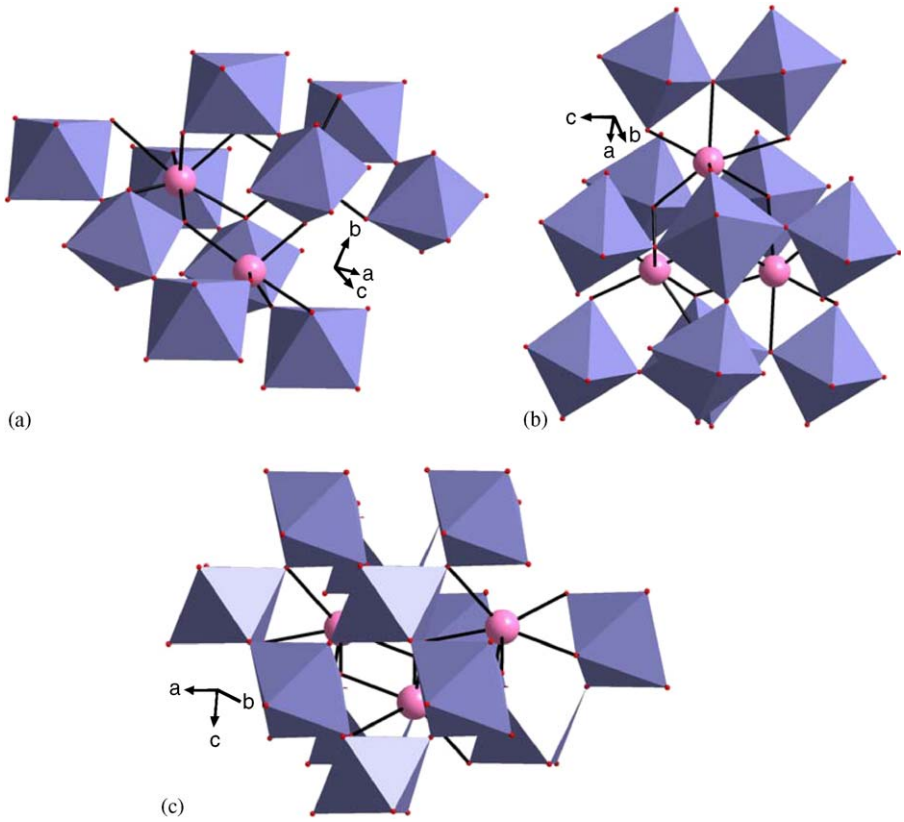

Fig. 3. The arrangement of (Nb/Ta)O_6 octahedra around a Bi_2O_2 unit in the triclinic forms of (a) $BiNbO_4$, (b) $BiTaO_4$ and orthorhombic form of (c) $BiNbO_4$.

There are two kinds of (Nb/Ta)O_6 octahedra. The Nb(1)O_6 and Nb(2)O_6 octahedra in $BiNbO_4$ are connected to each other along the *b*- and *c*-axis. Nb(1) is linked to Nb(2) along the *b*-axis via the axial oxygen atoms, O(3) and O(5), while along the *c*-axis, the octahedra occur as puckered sheets in a zigzag manner. The oxygen atoms, O(1) and O(7) of Nb(1)O_6 octahedra which are adjacent (*cis*) with respect to each other are free. These types of octahedral sheets, in which two vertices on each octahedron are *cis*, were first reported in the orthorhombic modification of $BiNbO_4$ [14]. Similar sheets are found in the monoclinic form of $NaNbO_2F_2$ [15] and in the orthorhombic forms of $BaMF_4$ where $M = Mn$, Co, Ni, and Zn [16–18]. In $BiTaO_4$, the TaO_6 octahedra are connected to each other along both *b*- and *c*-axis. Along the *c*-axis, the Ta(1)O_6 octahedron is connected to Ta(2)O_6 octahedron by corner sharing via the axial O(2) and O(8) atoms while along the *b*-axis, the octahedra are corner shared via the equatorial O(1) and O(6) atoms. The TaO_6 sheets are puckered along the *c*-axis in a zigzag fashion.

The main difference between the structures of $BiNbO_4$ and $BiTaO_4$ is that in $BiTaO_4$, two Ta(1)O_6 octahedra are linked through two of their adjacent edges to the [Bi_2O_2] units. The arrangement of NbO_6 octahedra around the [Bi_2O_2] units in the orthorhombic polymorph of $BiNbO_4$ is shown in Fig. 3c, where the [Bi_2O_2] units are surrounded by six NbO_6 octahedra via their edges. Thus, the triclinic and orthorhombic polymorphs of Bi(Nb/Ta)O_4 are structurally related. The ordered arrangement of (Nb/Ta)O_6 octahedra in the orthorhombic modification becomes puckered to give rise to a zigzag arrangement at higher temperature in the triclinic form. Further, the tilting of [Bi_2O_2] units in the triclinic form is due to an irregular co-ordination around Bi atoms owing to the presence of the $6s^2$ lone pair.

3.2. Photocatalysis

Earlier studies on the photocatalytic degradation of dyes by lithium bismuth niobate, $LiBi_4Nb_3O_{14}$ indicated selectivity towards quinonic dyes [19]. In order to check if $BiNbO_4$ also shows selectivity in the photodegradation of dyes, the degradation of azoic, quinonic and amino dyes such as OG, AG and MV, respectively, was investigated. The photocatalytic degradation of OG and AG was performed in the presence of both $BiNbO_4$ and $BiTaO_4$, initially. Fig. 4 shows the normalized degradation profiles of OG and AG in the presence of photocatalysts, $BiNbO_4$ and $BiTaO_4$. A total of 25 ppm solutions of OG and AG in the presence of 1 kg/m^3 of the catalysts were used for degradation. The degradation rate of OG was found to be faster than AG in the presence of $BiNbO_4$. However, the degradation of AG was faster than that of OG in the presence of $BiTaO_4$.

Table 3
Selected bond distances of (a) $BiNbO_4$ and (b) $BiTaO_4$

(a) $BiNbO_4$			
Bi(1)–O(1)	2.192 (4)	Bi(2)–O(1)	2.195 (4)
Bi(1)–O(2)	2.167 (4)	Bi(2)–O(1′)	2.770 (5)
Bi(1)–O(2′)	2.934 (4)	Bi(2)–O(2)	2.348 (4)
Bi(1)–O(4)	2.675 (5)	Bi(2)–O(3)	2.596 (4)
Bi(1)–O(5)	2.703 (5)	Bi(2)–O(7)	2.386 (4)
Bi(1)–O(7)	2.274 (4)	Bi(2)–O(7′)	2.706 (4)
Bi(1)–O(8)	2.477 (4)	Bi(2)–O(8)	2.248 (5)
Nb(1)–O(1)	2.175 (4)	Nb(2)–O(2)	2.046 (4)
Nb(1)–O(3)	1.840 (4)	Nb(2)–O(3)	2.190 (4)
Nb(1)–O(4)	1.963 (5)	Nb(2)–O(4)	1.958 (5)
Nb(1)–O(5)	2.224 (4)	Nb(2)–O(5)	1.833 (4)
Nb(1)–O(6)	1.859 (4)	Nb(2)–O(6)	2.057 (4)
Nb(1)–O(7)	1.981 (4)	Nb(2)–O(8)	1.910 (5)
(b) $BiTaO_4$			
Bi(1)–O(2)	2.65 (3)	Bi(2)–O(3)	2.24 (4)
Bi(1)–O(3)	2.32 (4)	Bi(2)–O(4)	2.34 (3)
Bi(1)–O(3′)	2.74 (4)	Bi(2)–O(5)	2.40 (3)
Bi(1)–O(4)	2.40 (2)	Bi(2)–O(6)	2.69 (5)
Bi(1)–O(4′)	2.74 (3)	Bi(2)–O(7)	2.86 (4)
Bi(1)–O(5)	2.35 (3)	Bi(2)–O(7′)	2.09 (4)
Bi(1)–O(7)	2.53 (3)	Bi(2)–O(8)	2.84 (5)
Ta(1)–O(1)	2.00 (4)	Ta(2)–O(1)	2.12 (4)
Ta(1)–O(2)	2.09 (8)	Ta(2)–O(2)	1.90 (8)
Ta(1)–O(3)	2.19 (4)	Ta(2)–O(5)	2.01 (2)
Ta(1)–O(4)	2.07 (3)	Ta(2)–O(6)	2.07 (5)
Ta(1)–O(6)	2.05 (5)	Ta(2)–O(7)	2.17 (4)
Ta(1)–O(8)	2.12 (5)	Ta(2)–O(8)	1.89 (5)

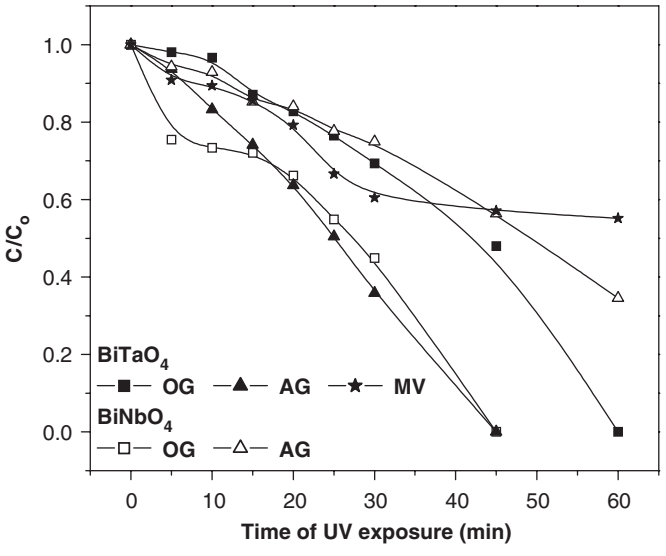

Fig. 4. Photocatalytic degradation profiles of the dyes, OG, MV and AG in the presence of $BiNbO_4$ and $BiTaO_4$.

The rate of degradation of MV in the presence of $BiTaO_4$ was the slowest among the three dyes investigated. It is interesting to note that no degradation of MV was observed in the presence of $BiNbO_4$ even after 1 h of UV radiation. This indicates that $BiNbO_4$ shows affinity towards quinonic and azo containing dyes and hence exhibits selectivity in degradation similar to an earlier study [19]. The powder X-ray patterns of both the catalysts show no change after degradation. Also, these materials possess very small surface areas of less than 1 m^2/g [19] (owing to their syntheses via the ceramic route) and therefore there is no adsorption of dyes on the catalysts. The difference in degradation rates of the dyes in presence of $BiTaO_4$ and $BiNbO_4$, is however, not apparent even though the band gaps of these materials are similar [6].

4. Conclusion

The crystal structures of the high temperature polymorphs of two important photocatalytic materials, $BiNbO_4$ and $BiTaO_4$ were re-determined by single-crystal X-ray diffraction. Both the compounds are iso-structural and consist of layers of $[Bi_2O_2]$ units separated by pseudo-layers of puckered sheets of Nb/TaO_6 octahedra. The crystal structures depict subtle variations with respect to co-ordination of the $(Nb/Ta)O_6$ octahedra around $[Bi_2O_2]$ units. The low-temperature orthorhombic and high temperature polymorphs are structurally related to each other in terms of the presence of layers of $[Bi_2O_2]$ units. Photocatalytic studies on the degradation of dyes indicate selectivity of $BiNbO_4$ towards aromatics containing quinonic and azo functional groups similar to that observed in $LiBi_4Nb_3O_{14}$.

Acknowledgments

Single-crystal X-ray data collection on the CCD facility under the IRPHA-DST program at the Indian Institute of Science is gratefully acknowledged. B. Muktha thanks CSIR for senior research fellowship.

References

[1] B. Aurivillius, Arkiv. Kemi. 3 (1951) 153.
[2] R.S. Roth, J.L. Waring, J. Res. Nat. Bur. Stand. Section A 66 (1962) 451.
[3] R.S. Roth, R.S. Waring, Am. Mineralogist 48 (1963) 1348.
[4] M.A. Subramanian, J.C. Calabrese, Mater. Res. Bull. 28 (1993) 523.
[5] E.T. Keve, A.C. Skapski, J. Solid State Chem. 8 (1973) 159.
[6] Z. Zou, J. Ye, H. Arakawa, Solid State Commun. 119 (2001) 471.
[7] C.-Y. Lee, R. Macquart, Q. Zhou, B.J. Kennedy, J. Solid State Chem. 174 (2003) 310.
[8] Z. Zou, J. Ye, K. Sayama, H. Arakawa, Chem. Phys. Lett. 343 (2001) 303.
[9] Z. Zou, H. Arakawa, J. Ye, J. Mater. Res. 17 (2002) 1446.
[10] G.M. Sheldrick, SHELXL97. Program for Crystal Structure Refinement, University of Gottingen, Germany, 1997.
[11] V. Petricek, M. Dusek, Jana 2000. Structure Determination Software Programs, Institute of Physics, Praha, Czech Republic, 2000.
[12] G. Sivalingam, K. Nagaveni, M.S. Hegde, G. Madras, Appl. Catal. B: Environ. 45 (2003) 23.
[13] W. Jeitschko, A.W. Sleight, Acta Crystallogr. B 30 (1974) 2088.

[14] E.T. Keve, A.C. Skapski, Chem. Commun. (1967) 281.
[15] S. Andersson, J. Galy, Acta Crystallogr. B 25 (1969) 847.
[16] E.T. Keve, S.C. Abrahams, J.L. Bernstein, J. Chem. Phys. 51 (1969) 4928.
[17] H.G. von Schnering, P. Blackmann, Naturwiss 55 (1968) 342.
[18] J.K. Brandon, H.D. Megaw, Philos. Mag. 21 (1970) 189.
[19] B. Muktha, M.H. Priya, M. Giridhar, T.N. Guru Row, J. Phys. Chem. B 109 (2005) 11442.